Systemic Elevation of PTEN Induces a Tumor-Suppressive Metabolic State

Isabel Garcia-Cao,[1] Min Sup Song,[1,9] Robin M. Hobbs,[1,7,9] Gaelle Laurent,[2,9] Carlotta Giorgi,[3,9] Vincent C.J. de Boer,[2] Dimitrios Anastasiou,[4] Keisuke Ito,[1] Atsuo T. Sasaki,[4] Lucia Rameh,[5] Arkaitz Carracedo,[1,8] Matthew G. Vander Heiden,[6] Lewis C. Cantley,[4] Paolo Pinton,[3] Marcia C. Haigis,[2] and Pier Paolo Pandolfi[1,*]

[1]Cancer Genetics Program, Beth Israel Deaconess Cancer Center, Departments of Medicine and Pathology, Beth Israel Deaconess Medical Center, Harvard Medical School, Boston, MA 02215, USA
[2]Department of Cell Biology, Paul F. Glenn Laboratories for the Biological Mechanisms of Aging, Harvard Medical School, Boston, MA 02115, USA
[3]Department of Experimental and Diagnostic Medicine, Section of General Pathology, Interdisciplinary Center for the Study of Inflammation (ICSI) and LTTA center, University of Ferrara, 44100 Ferrara, Italy
[4]Department of Systems Biology, Department of Medicine, Division of Signal Transduction, Beth Israel Deaconess Medical Center, Harvard Medical School, Boston, MA 02115, USA
[5]Boston Biomedical Research Institute, 64 Grove Street, Watertown, MA 02472, USA
[6]Koch Institute for Integrative Cancer Research at MIT, Cambridge, MA 02139, USA
[7]Present address: Australian Regenerative Medicine Institute and Monash Immunology and Stem Cell Laboratories, Monash University, Clayton, VIC 3800, Australia
[8]Present address: CIC bioGUNE, Technology Park of Bizkaia, 48160 Derio, Bizkaia, Spain and IKERBASQUE, Basque Foundation for Science, 48011 Bilbao, Bizkaia, Spain
[9]These authors contributed equally to this work
*Correspondence: ppandolf@bidmc.harvard.edu
DOI 10.1016/j.cell.2012.02.030

SUMMARY

Decremental loss of PTEN results in cancer susceptibility and tumor progression. PTEN elevation might therefore be an attractive option for cancer prevention and therapy. We have generated several transgenic mouse lines with PTEN expression elevated to varying levels by taking advantage of bacterial artificial chromosome (BAC)-mediated transgenesis. The "Super-PTEN" mutants are viable and show reduced body size due to decreased cell number, with no effect on cell size. Unexpectedly, PTEN elevation at the organism level results in healthy metabolism characterized by increased energy expenditure and reduced body fat accumulation. Cells derived from these mice show reduced glucose and glutamine uptake and increased mitochondrial oxidative phosphorylation and are resistant to oncogenic transformation. Mechanistically we find that PTEN elevation orchestrates this metabolic switch by regulating PI3K-dependent and -independent pathways and negatively impacting two of the most pronounced metabolic features of tumor cells: glutaminolysis and the Warburg effect.

INTRODUCTION

PTEN, a tumor suppressor frequently mutated or deleted in human cancer, is a main negative regulator of the phosphoinositide 3-kinase (PI3K) signaling pathway by dephosphorylating the 3′ position of phosphatidylinositol-3,4,5-trisphosphate (PIP_3) (Maehama and Dixon, 1998). The PI3K pathway transduces intracellular signals for growth, proliferation, and cell survival (Leevers et al., 1999). Somatic inactivation of *PTEN* occurs in a wide range of tumors, including glioblastoma, melanoma, prostate, and endometrial neoplasia (Bonneau and Longy, 2000; Cantley and Neel, 1999; Simpson and Parsons, 2001). Furthermore, germline mutations of *PTEN* are the underlying genetic cause of three related multiple hamartoma disorders: Cowden disease, characterized by an increased risk of breast and thyroid cancers; Bannayan-Zonana syndrome; and Proteus syndrome (Eng, 2003). Homozygous deletion of *Pten* in mice results in embryonic lethality, and *Pten* heterozygous mutant mice develop dysplasia in a wide spectrum of tissues and have a high incidence of prostate and colon tumors (Di Cristofano et al., 1998; Podsypanina et al., 1999; Suzuki et al., 1998). It has been previously reported that PTEN dose is a key determinant in prostate cancer progression (Trotman et al., 2003). Interestingly, a more recent study shows that even a slight reduction in PTEN levels dictates cancer susceptibility (Alimonti et al., 2010). These studies highlight the crucial dose-dependent role of PTEN in cancer progression.

Studies in *Drosophila melanogaster* reveal a novel role for PTEN in the control of tissue growth (Gao et al., 2000; Goberdhan et al., 1999; Huang et al., 1999). The phenotypes of flies carrying mutations for various components of the PI3K-PKB/Akt pathway have shown that this pathway positively controls cell number and cell size (Böhni et al., 1999; Scanga et al., 2000; Verdu et al., 1999; Weinkove et al., 1999). Consistent with its role as an antagonist of this pathway, *Drosophila* PTEN (dPTEN) loss-of-function mutants display increased cell and organ size, whereas overexpression of dPTEN yields the opposite phenotype.

Although consequences of gradual PTEN loss have been extensively studied, the consequences and potential benefits of elevating PTEN in the whole organism remain unknown. It has been reported in *Drosophila* that ubiquitous overexpression of PTEN results in lethality during embryonic and larval stages (Gao et al., 2000; Huang et al., 1999). Importantly, the tumor suppressor PTEN maintains cellular homeostasis through the regulation of biological processes both in the cytoplasm and within the nucleus (Salmena et al., 2008). However, it is currently unknown whether fluctuations in PTEN dose would impact its nuclear functions and/or its ability to modulate metabolic cues at the organismal level. This information is critically needed, as the elevation of PTEN is in principle an option for tumor prevention and therapy.

Tumor cells have a metabolism that is remarkably different from that in normal differentiated cells. Transformed cells take up and metabolize nutrients such as glucose and glutamine at high levels that support anabolic growth (Tong et al., 2009). In contrast to normal differentiated cells that rely primarily on mitochondrial oxidative phosphorylation to generate energy needed for cellular processes, most cancer cells instead rely on aerobic glycolysis, a phenomenon termed "the Warburg effect" (Warburg, 1956). The metabolic alterations and adaptations of cancer cells create a phenotype that is essential for tumor cell growth and survival, altering flux along key metabolic pathways such as glycolysis and glutaminolysis. Indeed there is mounting evidence for the therapeutic potential of targeting cancer metabolic reprogramming (Tennant et al., 2010).

Here we report that PTEN elevation is unexpectedly compatible with adult life and triggers a systemic metabolic regrogramming that results in a healthy and tumor-suppressive anti-Warburg state through the modulation of both PI3K-dependent and -independent pathways.

RESULTS

Generation of Super-PTEN Mice

To elucidate the pathophysiological impact of PTEN elevation, we attempted to generate transgenic (TG) mice carrying additional copies of this critical tumor suppressor gene (referred to as Super-PTEN mice). To maintain the regulation properties of the endogenous *Pten* gene, we made use of large genomic fragments containing the entire *Pten* locus carried by bacterial artificial chromosomes (BACs). These large genomic fragments protect the gene of interest from chromatin positional effects, preserving in every respect the pattern of expression of the endogenous gene. A genomic insert containing *Pten* (Figure 1A) was isolated from a mouse BAC genomic library. We obtained different TG lines containing varying numbers of the entire *Pten* locus. We next generated mouse embryonic fibroblasts (MEFs) from these lines to determine the PTEN expression level, which we found to vary from 1.1- to 3.5-fold above the endogenous level (Figures 1B and 1C).

PTEN Regulates Mammalian Body Size by Controlling Cell Number but Not Cell Size

Surprisingly, elevation of PTEN levels in the mouse was compatible with life but resulted in reduced body weight and size, a phenotype that was already evident during embryonic development (Figure 1D). Increased PTEN levels were observed in all adult tissues analyzed as well as during embryogenesis (Figure 1E) with no changes in its subcellular distribution and expression pattern (Figures 1F and 1G). All organs examined from TG mice with high PTEN levels weighed below normal, whereas the ratio of their weight to whole body weight was indistinguishable from that observed in wild-type (WT) individuals (Figure S1A available online). Serum leptin, GH, and IGF-1 levels were normal in Super-PTEN mice, therefore indicating that the effect of PTEN on body size is unlikely to be mediated indirectly through effects on hormone production (Figure S1B).

Interestingly, the effect on body weight and size (Figures 2A and 2C) was more severe as PTEN levels increased, revealing that PTEN controls body size in a dose-dependent manner in a mammalian organism (Figures 2A and 2B).

A reduction in organ size can be the result of a decrease in cell size, cell number, or both. Flow-cytometry analysis on dissociated cells from tissues (TG mice from line 3) revealed normal cell size (as measured by forward scatter), whereas the total number of cells was decreased (Figure 2D). Thus, PTEN elevation results in a reduced body size in mammals due to reduced cell number, with no effect on cell size.

PTEN Elevation Results in Reduced Cell Proliferation and Decreased c-Myc Levels and Confers Cancer Resistance

PTEN regulates a variety of biological processes to ensure correct cell homeostasis, and alterations of these functions contribute to cancer initiation and progression (Salmena et al., 2008). In line with this notion and with our previous results, Super-PTEN MEFs showed a significantly slower growth rate than their WT counterparts (Figures 3A and 3B: growth curve and serial 3T3 cultivation). The ability of primary MEFs to form colonies when seeded at low density is a reliable way to measure their proliferative potential. Indeed, Super-PTEN MEFs display a lower plating efficiency than those derived from WT embryos (Figure 3C).

We next examined the impact of PTEN overexpression on oncogene-mediated cellular transformation. Employing classical focus-formation assays with E1A and Ras oncogenes in Super-PTEN and WT MEFs, we found the number of foci of morphologically transformed cells in Super-PTEN cells to be decreased (Figure 3D). To validate this result in vivo, we evaluated the susceptibility of Super-PTEN mice to develop tumors upon chemical carcinogenesis (induction of fibrosarcomas by injection of 3MC, 3-methyl-cholantrene). As shown in Figure 3E, WT mice started developing tumors at week 14 after 3MC injection, whereas Super-PTEN mice developed tumors with a significantly longer latency, starting at week 21. It has been observed that 3MC treatment induces the methylation and corresponding loss of expression of tumor suppressor genes in rats (Liu et al., 2010). However, PTEN expression is maintained in 3MC-induced tumors from both WT and Super-PTEN mice (Figure 3E; western blot), suggesting that the tumor resistance phenotype of Super-PTEN mice is due to an enhanced PTEN-dependent tumor-suppressive effect rather than a reduced chance for *Pten* inactivation by 3MC. These data demonstrate that it is
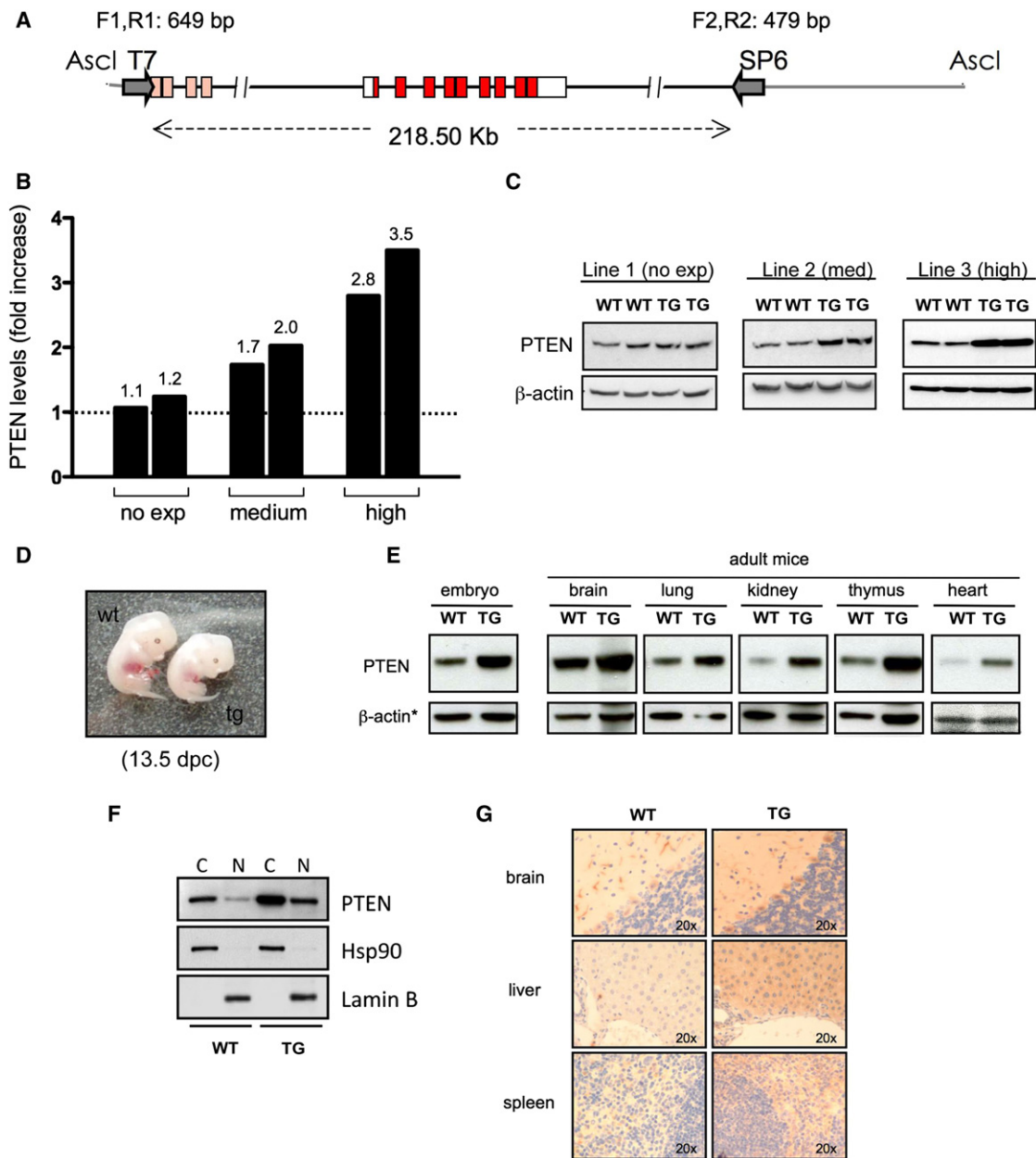
Figure 1. Generation of Super-PTEN Mice

(A) Map of the genomic insert carried by BAC RP23-215F15 clone (RPCI library, C57BL/6J) used to generate mice with increased gene dosage of PTEN ("Super-PTEN" mice). The genomic insert is 218.50 Kb long and contains the entire *Pten* locus (red boxes represent PTEN-coding sequence). Gray lines indicate the BAC vector (pBACe3.6) sequence. AscI was used to linearize the BAC clone. Primers used for detection of the transgene are shown (T7 side: F1,R1; SP6 side: F2,R2).

(B) Quantification of PTEN levels in the different BAC-PTEN TG lines generated. MEFs were obtained from each line, and total protein lysates were probed with antibodies toward PTEN and β-actin. The graph shows the fold increase in PTEN levels in each TG line relative to WT littermates.

(C) Representative immunoblotting of MEFs derived from lines with no expression (line 1), moderate expression (line 2), or high expression of the transgene (line 3).

(D) Representative images of WT and TG embryos harvested at 13.5 days post-coitum (dpc). Note reduced body size in TG embryo compared to WT.

(E) Western blot showing PTEN expression during embryogenesis and in tissues from adult mice (WT and TG from line 3). *In the case of heart, Ponceau S staining is shown as loading control.

(F) Western blot showing PTEN levels in cytoplasmic (C) and nuclear (N) extracts from WT and TG MEFs (line 3).

(G) PTEN expression by immunohistochemistry in tissues from WT and TG mice (line 3).
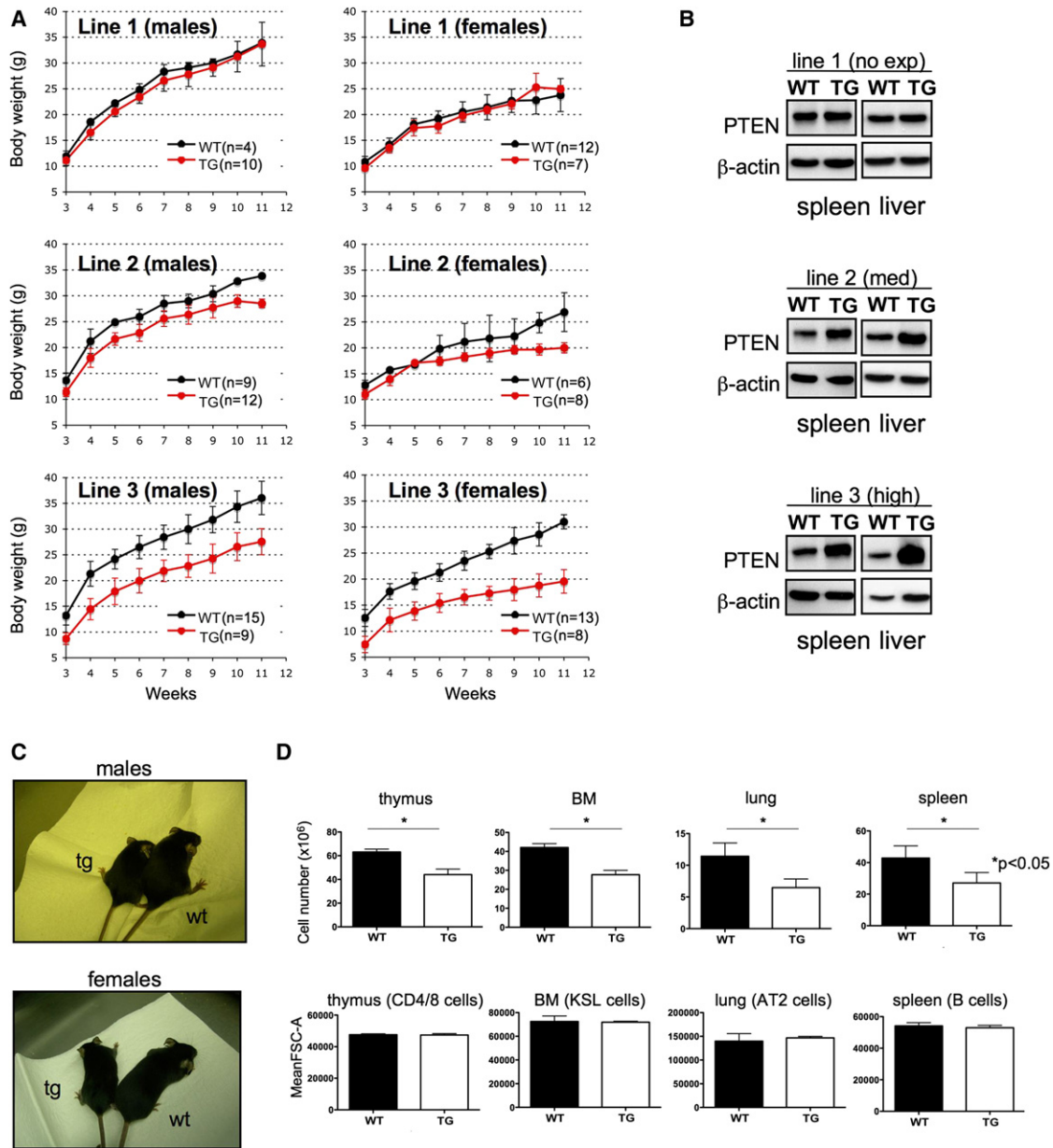
Figure 2. A Super-PTEN State Is Compatible with Life but Results in Decreased Organ Size due to Reduced Cell Number

(A) Growth curves indicate that PTEN overexpression results in reduced body mass. Note that the effect is more severe as PTEN dose increases.

(B) Western blot showing PTEN levels in different tissues (spleen, liver) from different PTEN TG lines (line 1: 1.2-fold; line 2: 2-fold; line 3: 3.5-fold above the endogenous PTEN level).

(C) Effect of PTEN overexpression on body size (line 3).

(D) Cell number and cell size in organs isolated from Super-PTEN and WT mice (line 3, n = 3 per genotype). BM = bone marrow. FSC = forward scatter. CD4/8 cells: CD4$^+$/Cd8$^+$, KSL cells: Lin$^-$/c-Kit$^+$/Sca-1$^+$, AT2 cells: Sca1$^-$/CD45$^-$/PECAM$^-$/Autofl^{hi}, B cells: B220^{mid+}/IgM^{mid+}.

Error bars in (A) and (D) denote standard deviation (SD). See also Figure S1.

possible to confer resistance to oncogenic transformation both in vitro and in vivo by increasing PTEN levels.

The reduced organ weight, size, and cellularity observed in Super-PTEN mice were reminiscent of the phenotype observed in *c-Myc* hypomorphic mice (Trumpp et al., 2001). c-Myc plays a key role in direct reprogramming of somatic cells into induced

pluripotent stem cells (iPSCs) (Banito and Gil, 2010). iPSC reprogramming is achieved by coexpressing pluripotency factors and oncogenes, including c-Myc, and can provide a readout of transformability and oncogenic potential (Banito and Gil, 2010), whereas it has been recently reported that tumor suppressors act as a barrier to reprogramming (Banito et al., 2009; Hong
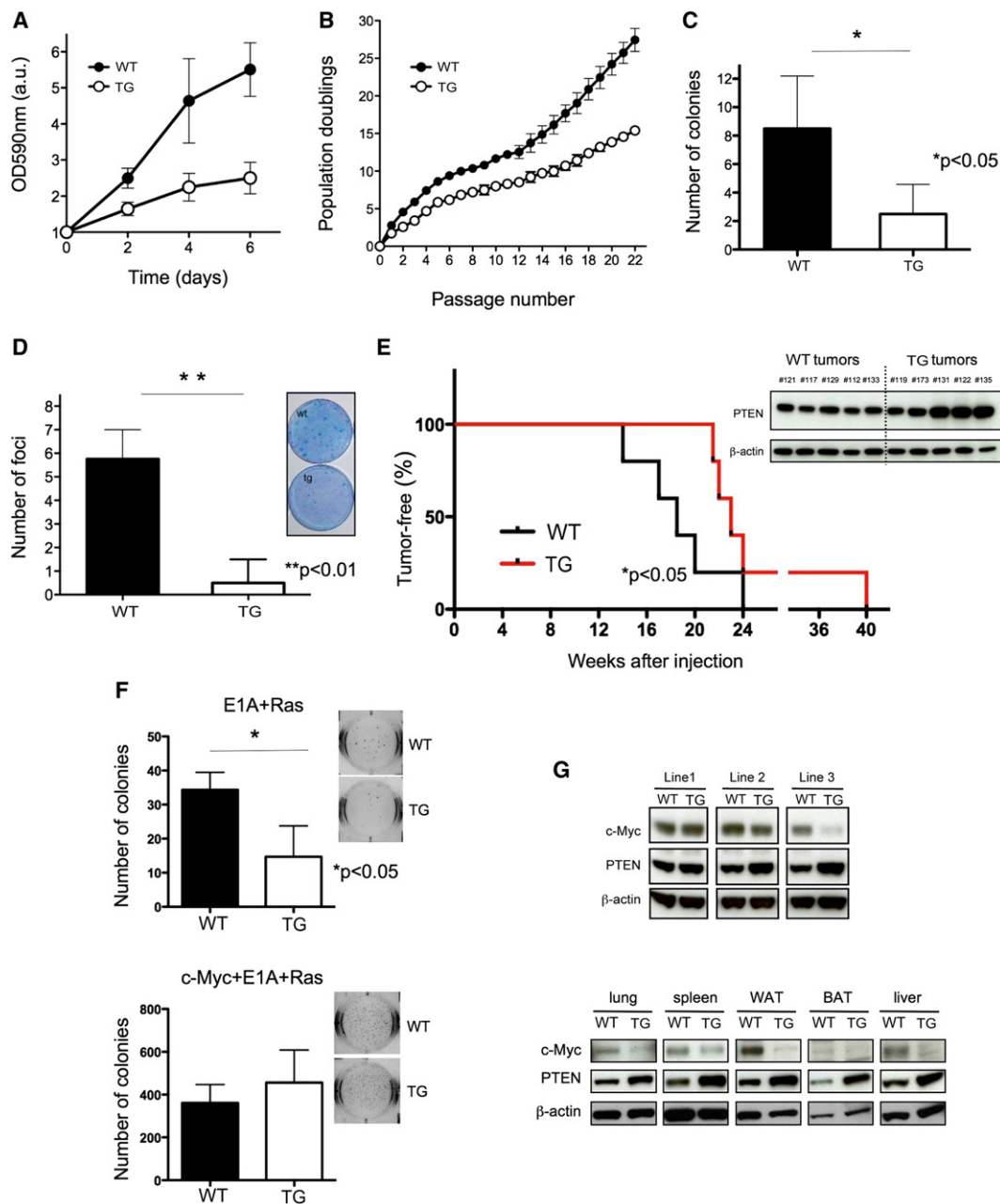
Figure 3. PTEN Overexpression Results in Reduced Growth Rate in Culture, Resistance to Oncogenic Cellular Transformation, and Decreased c-Myc Levels and Confers Cancer Resistance In Vivo

(A) Growth curves of WT and TG MEFs (n = 3 per genotype).

(B) Serial 3T3 cultivation of primary WT and TG MEFs (n = 3). The figure shows the accumulated population doublings (PDL) at each passage.

(C) Colony-formation efficiency of WT and TG MEFs (n = 4).

(D) Transformation susceptibility of WT and TG MEFs (n = 4). The picture shows the numbers of neoplastic foci formed after transfection with a combination of oncogenic Ras and E1A.

(E) Susceptibility to 3MC-induced fibrosarcomas. Mice of the indicated genotypes were injected intramuscularly with 3MC in one of the rear legs, and the latency for the development of fibrosarcomas was scored (line 3, n = 5 per genotype). Super-PTEN mice developed tumors with a significantly longer latency than WT mice, as determined by Gehan-Breslow-Wilcoxon test (*p < 0.05). Western blot shows PTEN expression levels in tumors derived from WT and Super-PTEN mice.

(F) Soft-agar assay in primary MEFs transformed by E1A+Ras (top) or c-Myc+E1A+Ras (bottom). The graph shows the number of colonies per well (6-well plates, triplicate samples). A representative picture from the assay is shown.

(G) Immunoblotting of protein lysates from WT and TG MEFs (top) and tissues (bottom, mice from line 3). Total cell extracts were probed with antibodies toward c-Myc, PTEN and β-actin. WAT = white adipose tissue, BAT = brown adipose tissue.

Error bars in (A), (B), (C), (D), and (F) denote SD. See also Figure S2.

et al., 2009; Kawamura et al., 2009; Li et al., 2009; Marión et al., 2009; Utikal et al., 2009). Overexpression of PTEN in cells resulted in a reduced number of iPSC colonies upon expression of reprogramming factors *Oct4*, *Sox2*, and *Klf4* (Figure S2A), whereas, importantly, the negative effect of PTEN expression in iPSC formation was overcome by *c-Myc* transduction. To determine the involvement of c-Myc in the resistance of Super-PTEN cells to oncogenic transformation, we performed soft-agar assays to evaluate anchorage-independent growth in cells infected with E1A-Ras alone or in the presence of c-Myc (cMyc+E1A-Ras). As shown in Figure 3F (top), Super-PTEN cells form fewer colonies in soft agar when compared to WT cells. This resistance to transformation in Super-PTEN cells is completely rescued by the addition of c-Myc (Figure 3F, bottom). On the basis of these observations, we hypothesized that PTEN opposes c-Myc function or suppresses its expression. Indeed, c-Myc expression was profoundly reduced in various tissues both in Super-PTEN MEFs as well as in vivo (Figure 3G).

Super-PTEN Mice Exhibit Increased Energy Expenditure

We next examined the effect of a Super-PTEN state on body fat accumulation and energy metabolism. Given the inhibitory role of PTEN on signaling pathways critical for growth factors and glucose uptake (Leevers et al., 1999), we anticipated that Super-PTEN mice would exhibit reduced metabolic activity. Surprisingly, Super-PTEN mice exhibited reduced body fat accumulation compared to WT counterparts, as determined by EchoMRI (Figure 4A), suggesting that PTEN elevation impacts nutrient adaptation and utilization. Furthermore, indirect calorimetry analysis revealed that Super-PTEN mice presented higher energy expenditure than WT mice (Figures 4B and S3A), although locomotor activity was not significantly affected (Figure S3B). Food intake was similar or even slightly higher in Super-PTEN mice (Figure S3C), indicating that the difference in energy expenditure observed between WT and Super-PTEN mice is not due to changes in food intake and rather due to an elevated metabolic state.

FAO (fatty acid oxidation) represents a crucial process in energy metabolism and fat storage (Ruderman and Flier, 2001). Fatty acids can be either used for lipid synthesis and protein modification or degraded through mitochondrial β-oxidation, which produces substrates that maintain ATP generation through oxidative phosphorylation. To determine a potential contribution of altered FAO to the metabolic state of Super-PTEN mice and cells, we initially measured the expression levels of key enzymes in fatty acid metabolism (SCD1, CPT-1α, PPAR-α, PPAR-δ, PDK4, MCAD, Acox1). However, we could not find significant differences in the expression of these genes, with the exception of *Cpt-1α* (Figure S3D), which is slightly increased in Super-PTEN cells. Interestingly, PI3K signaling reportedly suppresses *Cpt-1α* expression (Deberardinis et al., 2006). We could not find significant differences in the rate of FAO between WT and Super-PTEN cells, either primary MEFs (Figure S3E) or hepatocytes (Figure S3F). We next examined the use of glucose as a precursor for lipid synthesis and found that Super-PTEN cells show a significant reduction in the contribution of (6-^{14}C)-glucose to lipid synthesis when compared to WT cells (Figure S3G). This decreased rate of lipogenesis is consistent with the reduction in body fat accumulation observed in Super-PTEN mice. We next evaluated serum lactate levels as an indicator of glycolytic activity in Super-PTEN mice. As shown in Figure 4C, we observed a reduction in lactate levels in Super-PTEN mice compared to WT littermates. Pyruvate generated from glucose catabolism can be reduced to lactic acid (anaerobic glycolysis) or further metabolized by the mitochondria (oxidative phosphorylation). These data suggested that the increase in energy expenditure observed in Super-PTEN mice could reflect increased mitochondrial oxidative phosphorylation and a concomitant reduction in anaerobic glycolysis.

PTEN Elevation Shifts Cellular Energy Metabolism toward Mitochondrial Respiration

To determine the contribution of mitochondrial respiration to cellular bioenergetics, we measured oxygen consumption in Super-PTEN and WT MEFs. The difference in energy expenditure in vivo was consistent with the increased mitochondrial oxygen consumption observed in primary Super-PTEN MEFs (Figure 5A), which was accompanied by increased mitochondrial ATP production (Figure 5B) and the generation of reactive oxygen species (ROS) (Figure S4A). It has previously been shown that hypoxia-inducible factor 1 (HIF-1) stimulates glycolytic energy production and negatively regulates mitochondrial biogenesis and O_2 consumption (Denko, 2008). Because activation of the PI3K-Akt pathway leads to increased HIF-1α levels and activity (Zundel et al., 2000), we compared the levels of HIF-1α in Super-PTEN versus WT MEFs. However, we found no substantial differences in HIF-1α protein levels (Figure S4B) or HIF-1α target genes (Figure S4C) between Super-PTEN and WT MEFs.

The increased mitochondrial ATP production could not be ascribed to a more efficient mitochondrial Ca^{2+} uptake (Griffiths and Rutter, 2009) as this parameter was if anything slightly lower in Super-PTEN MEFs (Figure 5C). Moreover, Super-PTEN and WT MEFs showed similar mitochondrial membrane potential ($\Delta\Psi_m$) (Figure 5D). Strikingly, however, Super-PTEN MEFs exhibited greater mitochondrial biogenesis. Indeed, total network mitochondrial volume was higher in Super-PTEN MEFs due to an increase in mitochondrial number, whereas average mitochondrial volume and morphology were unaffected (Figure 5E).

Microarray analysis revealed that Super-PTEN MEFs exhibited a significant PGC-1α gene enrichment signature (Figure S4D), consistent with the fact that Akt suppresses PGC-1α function (Li et al., 2007). PGC-1α is a key regulator of energy metabolism that promotes mitochondrial oxidative phosphorylation and mitochondrial biogenesis (Puigserver and Spiegelman, 2003; Wu et al., 1999).

To functionally assess differences in mitochondrial activity, we forced cells to rely on oxidative phosphorylation alone for energy production by substituting glucose for galactose in the growth media (Marroquin et al., 2007). In line with an increased mitochondrial function, Super-PTEN cells showed less of a reduction in growth in galactose versus glucose compared to WT cells (Figure S4E). Thus, through the generation of the Super-PTEN mouse we have identified a role for PTEN in energy homeostasis and mitochondrial biogenesis and function.
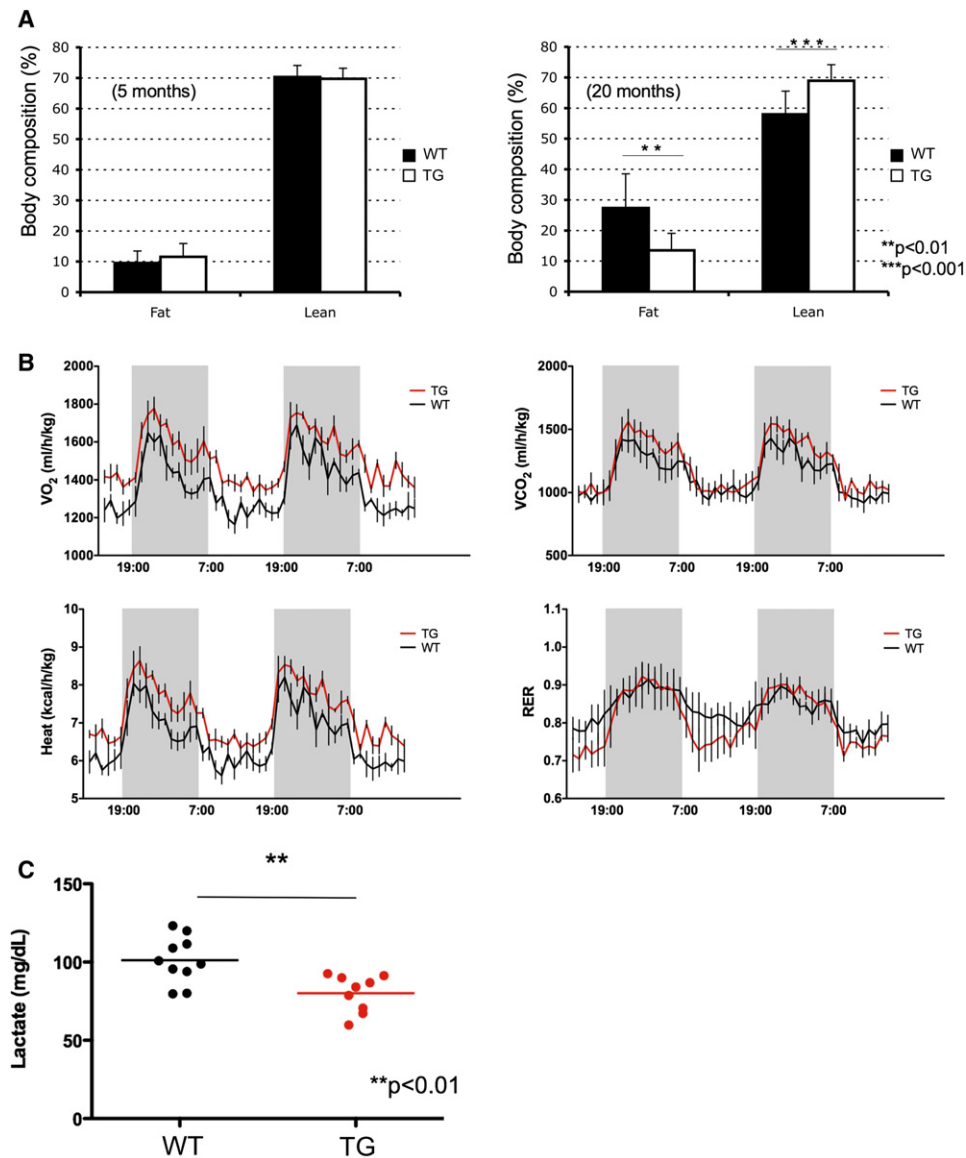
Figure 4. Super-PTEN Mice Show Increased Energy Expenditure
(A) Percentage of fat and lean mass was determined in young (left panel: WT, n = 7; TG, n = 7) and old mice (right panel: WT, n = 12; TG, n = 10) by EchoMRI (line 3).
(B) Indirect calorimetry of Super-PTEN (red line) and WT mice (black line). Oxygen consumption (VO_2), carbon dioxide release (VCO_2), respiratory exchange ratio (RER; VCO_2/VO_2), and energy expenditure per kg of body weight were determined in Super-PTEN and WT mice in metabolic chambers (line 3, n = 4 per genotype).
(C) Serum lactate levels in WT (n = 10) and TG (n = 9) mice (line 3).
Error bars in (A) denote SD; error bars in (B) denote standard error of the mean (SEM). See also Figure S3.

The Super-PTEN State Is Accompanied by Repressed PI3K-Akt Signaling and Reduced Glucose Uptake in Spite of High Energy Utilization

We then aimed to define the biochemical features of Super-PTEN mice that are responsible for this unexpected metabolic phenotype. PTEN is the main negative regulator of the PI3K pathway, a highly oncogenic and metabolic node (Engelman et al., 2006). Dephosphorylation of PIP_3 by PTEN impairs Akt activation and thereby opposes the PI3K-Akt signaling pathway.

Consistently, cells overexpressing PTEN show reduced levels of the substrate PIP_3 (Figure S5A), reduced PI3K activity (as measured by phosphorylation of the downstream component Akt) (Figure S5B), and impaired glucose uptake (Figure S5C). The analysis of glucose and lactate metabolites in the extracellular media revealed that Super-PTEN cells consume less glucose and extrude less lactate into the media than WT cells (Figure 6A). These data demonstrate that a Super-PTEN state is coherently accompanied by repressed PI3K-Akt signaling
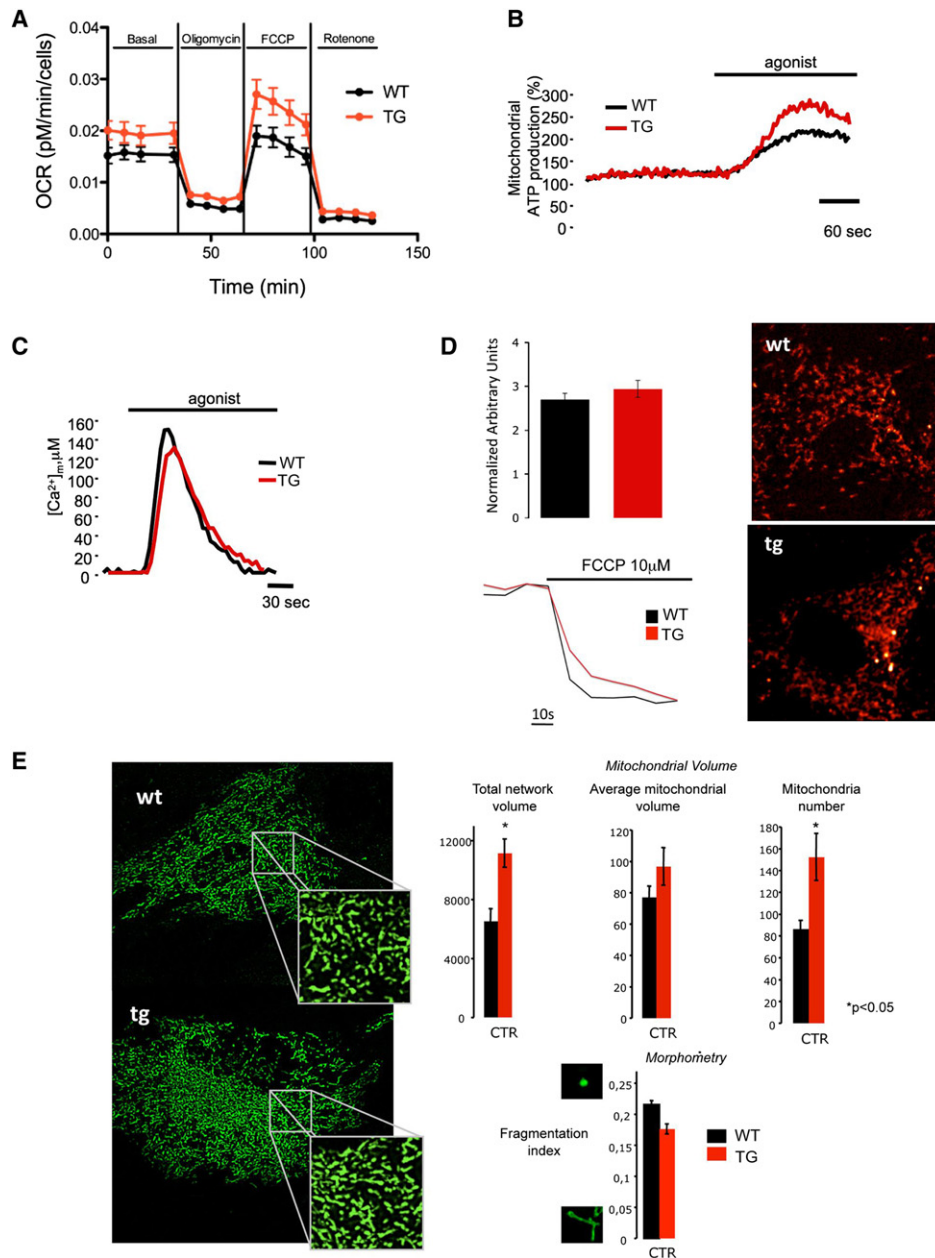
Figure 5. PTEN Overexpression Results in Increased Mitochondrial Oxygen Consumption, Mitochondrial ATP Production, and Mitochondrial Number

(A) OCR was measured (Seahorse XF24 analyzer) in primary WT and TG MEFs (n = 3 per genotype) under basal conditions and after addition of oligomycin, FCCP, and Rotenone.

(B) Mitochondrial ATP production in WT and TG MEFs after agonist stimulation as described in the Experimental Procedures. Where indicated, cells were treated with 100 μM ATP. Data are expressed as a percentage of the initial value. WT: 162% ± 8%; TG: 251% ± 18%. n = 15 from three independent experiments and p < 0.05 (mean ± SEM).

(C) Mitochondrial Ca^{2+} homeostasis measurements after agonist stimulation as described in the Experimental Procedures. Where indicated, cells were treated with 100 μM ATP. WT: $[Ca^{2+}]_m$ peak 155 ± 8 μM. TG: $[Ca^{2+}]_m$ peak 131 ± 5 μM. n = 12 from three independent experiments (mean ± SEM).

(D) Analysis of $\Delta\Psi_m$ in WT and TG MEFs. Cells where loaded with TMRM as described in the Experimental Procedures. Where indicated cells were treated with FCCP to collapse completely the $\Delta\Psi_m$. The traces are representative of single-cell responses (WT, n = 28; TG, n = 33).

(E) Analysis of total and single mitochondrial volume and mitochondrial numbers as described in the Experimental Procedures (WT, n = 43; TG, n = 40 from three independent experiments and p < 0.05). Mitochondrial morphology in WT and TG MEFs was revealed by mitochondrial targeted GFP visualization. Mitochondrial fragmentation index was calculated as described in the Experimental Procedures (WT, n = 43; TG, n = 40 from three independent experiments). Ordinates for the graphs of network volume, average mitochondrial volume, and mitochondrial number are voxel/cell, voxel/object, and N° object/cell, respectively.

Error bars in (A) denote SD; error bars in (D) and (E) denote SEM. See also Figure S4.
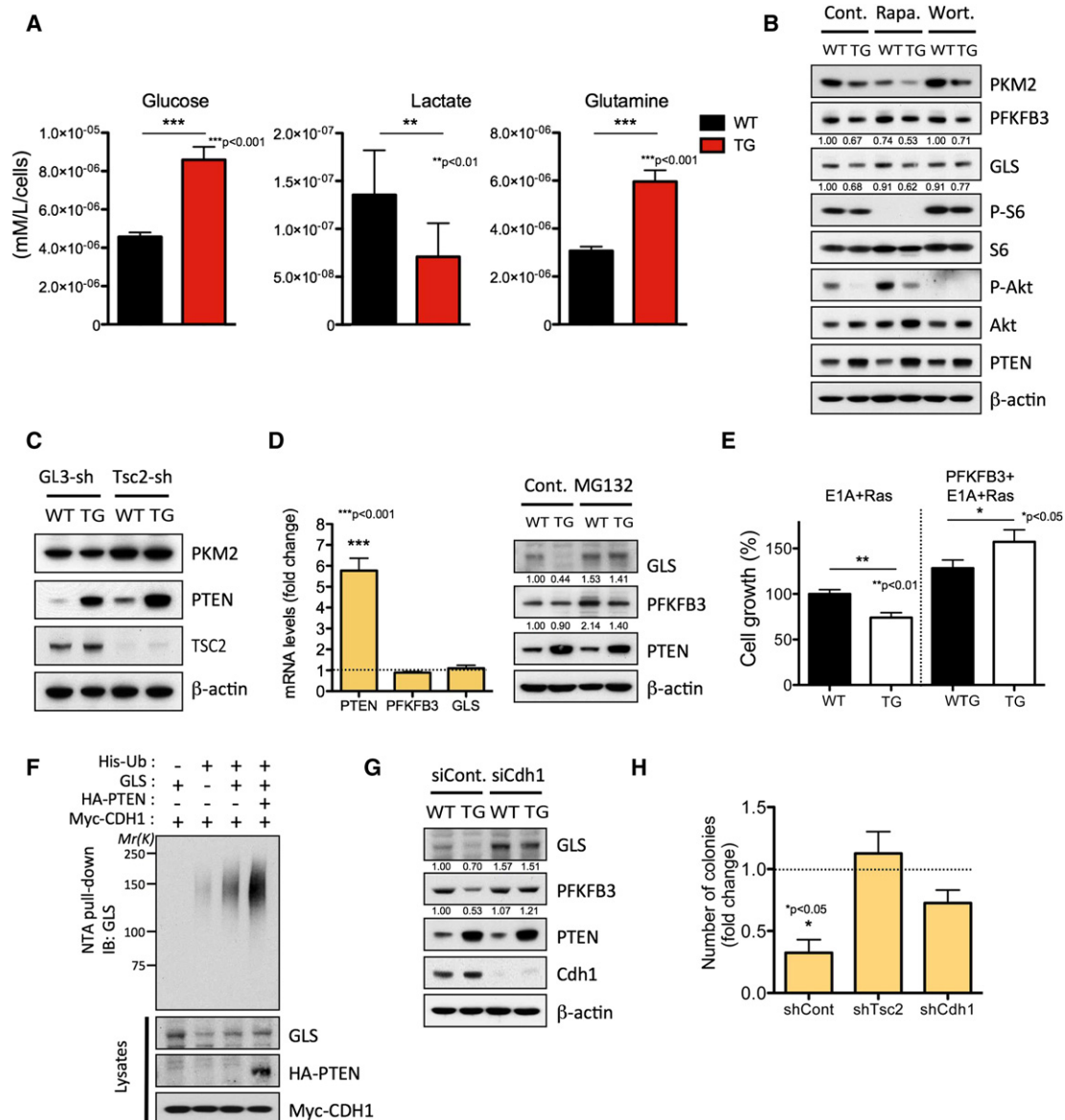
Figure 6. PTEN Elevation Induces a Tumor-Suppressive Metabolic State by Regulating PI3K-Dependent and -Independent Pathways

(A) Glucose, lactate, and glutamine levels in culture media were measured in WT and TG cells (n = 2) and normalized to cell number.

(B) Effects of pharmacological inhibition of mTORC1 and PI3K-Akt pathway on glycolytic and glutaminolytic enzymes. Cell lysates from WT and TG MEFs treated with DMSO (Cont.) or 20 nM rapamycin (Rapa.) for 24 hr or 100 nM wortmannin (Wort.) for 8 hr were subjected to immunoblotting with antibodies against PKM2, PFKFB3, GLS, p-S6, S6, p-Akt, Akt, PTEN, and β-actin.

(C) Effects of TSC2 depletion-mediated mTORC1 activation on PKM2 protein level. Cell lysates from GL3-shRNA (control shRNA against the luciferase gene) and *Tsc2*-shRNA infected WT and TG MEFs were subjected to immunoblotting with antibodies against PKM2, TSC2, PTEN, and β-actin.

(D) Fold change ratio (TG versus WT) in *Pten*, *Pfkfb3*, and *Gls* mRNA levels determined by qRT-PCR of total RNA from WT and TG MEFs (left). Proteasome-mediated degradation of GLS and PFKFB3 is shown. Cell lysates from WT and TG MEFs treated with 10 μM of the proteasome inhibitor MG132 for 4 hr were subjected to immunoblotting with antibodies against GLS, PFKFB3, PTEN, and β-actin (right).

(E) Impact of PFKFB3 overexpression in cell growth (48 hr after plating) in primary MEFs transformed by E1A+Ras. Percentage of growth relative to WT MEFs+E1A+Ras is shown.

(F) PTEN enhances APC/C-Cdh1-mediated ubiquitination of GLS. *PTEN*-deficient PC-3 cells were cotransfected with GLS, His-Ub, CDH1, and PTEN and treated with MG132 (10 μM) for 4 hr before harvesting. His-Ub-conjugated GLS was purified from cell lysates using an Ni^{2+}-NTA spin column under denaturing conditions.

(G) *Cdh1* silencing recovers the levels of GLS and PFKFB3 in TG MEFs. Cell lysates from WT and TG MEFs transfected with siRNAs for *Renilla* luciferase (siCont.) or *Cdh1* were subjected to immunoblotting with antibodies against GLS, PFKFB3, PTEN, Cdh1, and β-actin.

(H) Number of colonies (fold change ratio: TG versus WT MEFs+Ras) formed in soft-agar assay after *Tsc2* or *Cdh1* knockdown in immortalized TG MEFs transformed by oncogenic Ras.

Error bars in (A), (D), (E), and (H) denote SD. See also Figure S5.

and reduced glucose uptake. Although the prediction is that this would result in low energy utilization, it was surprisingly not the case in Super-PTEN cells and mice (see above).

PTEN Regulates PKM2 Levels through mTORC1

One key characteristic of cancer cells is the way glucose is utilized, switching from energy-efficient oxidative phosphorylation to inefficient lactate production (Warburg effect), allowing for the accumulation of glycolysis intermediates and their redirection to biosynthetic pathways. Our data show that Super-PTEN cells take up less glucose, and yet they redirect a greater fraction of glycolytic products into mitochondrial oxidative phosphorylation. These features could be regarded as an anti-Warburg status, which would correlate with decreased proliferation and a cancer-resistant state. One of the central components in the metabolic switch is the enzyme responsible for converting phosphoenolpyruvate into pyruvate, pyruvate kinase (PK). The switch from pyruvate kinase M 1 (PKM1) expression to PKM2 in cells results in a lower rate of PK activity, allowing the accumulation of glycolytic precursors for the production of redox power and biomass (Vander Heiden et al., 2009, 2010). We therefore studied the status of PKM2 in Super-PTEN cells. Interestingly, Super-PTEN cells had reduced levels of PKM2 (Figure 6B) and decreased PK activity (Figure S5D), suggesting that altered activity of this glycolytic regulatory node may contribute to the observed metabolic changes in Super-PTEN cells.

As the PKM1/M2 isoforms are generated through alternative splicing of two mutually exclusive exons (Christofk et al., 2008; Clower et al., 2010; David et al., 2010), we next compared splicing patterns of the *Pkm* gene in WT and Super-PTEN MEFs. However, *Pkm2* was the predominant mRNA isoform in MEFs regardless of genotype (Figure S5E). This result was unanticipated given that PKM2 splicing is under control of c-Myc (David et al., 2010) and that we find Super-PTEN cells to express lower levels of c-Myc (Figure 3G). Interestingly, in the iPSC reprogramming experiments, addition of c-Myc rescues PKM2 expression in Super-PTEN cells (Figure S2B). However, splicing pattern analysis (Figure S2C) suggests that the c-Myc-dependent rescue of PKM2 levels in Super-PTEN cells under iPSC reprogramming conditions is mediated through a mechanism distinct to a switch in splicing patterns (see below).

In an effort to account for changes to PKM2 expression in Super-PTEN cells, we investigated the potential involvement of other PTEN-regulated cellular pathways in the control of PKM2 expression. Rapamycin treatment was found to reduce PKM2 levels in MEFs, suggesting that decreased activity of mTORC1, a downstream target of the PI3K-Akt pathway (Zoncu et al., 2011), could account for the reduced levels of PKM2 in Super-PTEN cells (Figure 6B). To test this hypothesis, we analyzed PKM2 expression in WT and Super-PTEN MEFs upon knockdown of *Tsc2*, a negative regulator of mTORC1 (Tee and Blenis, 2005). Importantly, hyperactivation of the mTORC1 pathway by *Tsc2* knockdown rescued PKM2 levels in Super-PTEN MEFs and further increased PKM2 levels in WT cells (Figure 6C), confirming that reduced mTORC1 activity in Super-PTEN cells accounts for the decreased expression of PKM2. Interestingly, *Tsc2* knockdown also increased c-Myc expression in Super-

PTEN cells, although levels still remained substantially lower than those of WT cells (Figure S5F). These data are consistent with the described role of mTORC1 in regulating *c-Myc* translation (West et al., 1998). However, the inability of *Tsc2* knockdown to completely rescue c-Myc expression in Super-PTEN cells indicates that additional pathways downstream of PTEN known to regulate c-Myc levels are co-ordinately active (Gregory et al., 2003; Sears et al., 2000). Conversely, the ability of c-Myc to rescue PKM2 expression in Super-PTEN cells during iPSC reprogramming may be related to enhanced mTORC1 signaling at multiple levels (Jones et al., 1996; Ravitz et al., 2007).

PTEN Controls both Glycolysis and Glutaminolysis through Regulation of PFKFB3 and GLS Stability

The regulation of metabolism and growth must be tightly coupled to guarantee efficient use of energy and anabolic substrates throughout the cell cycle. PFKFB3 (6-phosphofructo-2-kinase/fructose-2,6-biphosphatase isoform 3) potently stimulates glycolysis by catalyzing the formation of fructose 2,6-bisphosphate, an allosteric activator of 6-phosphofructo-1-kinase (PFK-1), a rate-limiting enzyme and essential control point in glycolysis. PFKFB3 has been shown to be abundantly expressed in human tumors (Atsumi et al., 2002) and required for the high glycolytic rate and anchorage-independent growth of Ras-transformed cells (Telang et al., 2006). As shown in Figure 6B, PFKFB3 levels are downregulated in Super-PTEN cells.

Cancer cells depend on a high rate of glucose uptake and metabolism to maintain their viability despite being maintained in an oxygen-replete environment. Another remarkable metabolic feature of tumor cells is glutamine addiction. Interestingly, Super-PTEN cells show an impaired glutamine uptake (Figure 6A) and reduced levels of glutaminase (GLS), the first enzyme in the glutaminolysis pathway (Figure 6B). Therefore, PTEN elevation negatively impacts both glycolysis and glutaminolysis through the regulation of PFKFB3 and GLS.

Both GLS and PFKFB3 are substrates targeted for degradation by the E3 ubiquitin ligase anaphase-promoting complex/cyclosome-Cdh1 (APC/C-Cdh1) (Colombo et al., 2010; Najafov and Alessi, 2010), and PTEN has recently been demonstrated to promote APC/C-Cdh1 activity (Song et al., 2011). This function of PTEN is dependent on its ability to directly promote APC/C-Cdh1 complex assembly and independent of its ability to inhibit the PI3K signaling pathway through dephosphorylation of PIP_3. Consistently, both PFKFB3 and GLS levels were unaffected by treatment with the PI3K inhibitor wortmannin (Figure 6B). We found that the reduction in PFKFB3 and GLS levels was rescued by MG132 treatment, and no significant changes in mRNA levels were found in cells overexpressing PTEN compared to WT cells, indicating a proteasome-dependent downregulation of PFKFB3 and GLS (Figure 6D). Super-PTEN cells are resistant to transformation and show a reduced growth rate in response to the oncogenic combination E1A+Ras. Importantly, the addition of PFKFB3 is able to completely rescue the deficient growth of transformed Super-PTEN cells (Figure 6E). An in vivo ubiquitination assay confirmed GLS as a substrate for APC/C-Cdh1 and increased GLS ubiquitination in the presence of PTEN (Figure 6F). PFKFB3 and GLS levels were rescued by depletion of Cdh1 (Figure 6G),
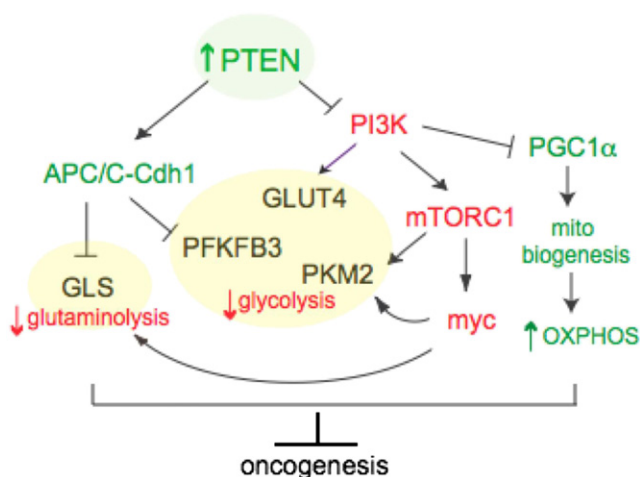
Figure 7. PTEN Induces a Tumor-Suppressive Metabolic State by Regulating PI3K-Dependent and -Independent Pathways
Model by which PTEN elevation negatively impacts two of the most noticeable metabolic features of tumor cells: glutaminolysis and the Warburg effect.

indicating that PTEN negatively regulates PFKFB3 and GLS through the APC/Cdh1 complex.

Reduced PKM2, PFKFB3, and GLS protein levels characterize the tumor-suppressive metabolic state of Super-PTEN cells. As discussed above, PKM2 levels are rescued by *Tsc2* knockdown (Figure 6C), whereas PFKFB3 and GLS levels are normalized by *Cdh1* inactivation (Figure 6G). As previously described (Li et al., 2008; Zhang et al., 2003), *Tsc2* or *Cdh1* knockdown resulted in a marked reduction in growth rate of primary MEFs (Figure S5G), although this effect was more pronounced with WT than with Super-PTEN cells in the case of *Tsc2* inactivation. To assess whether *Tsc2* or *Cdh1* inactivation could rescue the resistance to oncogenic transformation of Super-PTEN cells, we studied anchorage-independent growth of immortalized WT and Super-PTEN MEFs after introduction of oncogenic Ras. Strikingly, *Tsc2* inactivation renders Super-PTEN cells as susceptible to oncogenic transformation as WT cells, whereas *Cdh1* inactivation leads to a partial rescue in colony-forming ability in soft agar (Figure 6H).

On the basis of these findings, we propose a model (Figure 7) by which PTEN elevation induces a tumor-suppressive metabolic state by regulating PI3K-dependent and -independent pathways and negatively impacts two of the most noticeable metabolic features of tumor cells: glutaminolysis and the Warburg effect.

DISCUSSION

Our study reveals the profound impact of PTEN elevation in organismal homeostasis and cancer development. Studies in *D. melanogaster* have highlighted roles of the Akt pathway in positively controlling cell number and cell size (Böhni et al., 1999; Gao et al., 2000; Goberdhan et al., 1999; Huang et al., 1999; Scanga et al., 2000; Verdu et al., 1999; Weinkove et al., 1999). However, our data show that the reduction in organism and tissue size in

Super-PTEN is due solely to a reduction in cell number, not cell size. Interestingly, cell growth phenotypes of some *Drosophila* mutations are not always paralleled by their mammalian counterparts. For instance, reduction of c-Myc expression in mice results in an overall decrease in body size due to a reduction in cell number (hypoplasia) without detectable changes in cell size (Trumpp et al., 2001), whereas *Drosophila dmyc* mutants are smaller as a result of reduced cell size (hypotrophy) (Johnston et al., 1999). Our Super-PTEN model displays an obvious reduction of c-Myc expression as well, yet reduced cell number but not cell size is the outcome at the organismal level. Nevertheless, the c-Myc downregulation is a distinctive component of the Super-PTEN phenotype. Accordingly, c-Myc overexpression rescues the defective three-factor iPSC reprogramming of Super-PTEN MEFs. Further, c-Myc controls genes regulating glucose metabolism and glutaminolysis, including PKM2 and GLS, which are decreased in Super-PTEN cells (David et al., 2010; Gao et al., 2009).

Tumor cells exhibit an altered metabolism that allows them to sustain higher proliferative rates and resist cell death signals (DeBerardinis et al., 2008; King and Gottlieb, 2009; Tennant et al., 2009). Microarray analysis revealed that genes of the glycolysis pathway are overexpressed in the majority of clinically relevant cancers (Altenberg and Greulich, 2004). Among these genes is PK, which regulates the rate-limiting final step of glycolysis. Recent work demonstrated that expression of the type II isoform of the *Pkm* gene is a critical determinant of the metabolic phenotype of cancer cells and confers a selective proliferative advantage to tumor cells in vivo (Christofk et al., 2008). Our data show that Super-PTEN cells have reduced levels of PKM2, and that this key regulator of glycolytic flux is under the control of the mTORC1 pathway. Another key regulator of glycolysis is PFKFB3, which potently stimulates glycolysis by catalyzing the formation of fructose 2,6-bisphosphate, the allosteric activator of PFK1 (Hue and Rider, 1987), a rate-limiting enzyme of glycolysis. It has been previously reported that PFKFB3 is constitutively expressed by neoplastic cells and serves as an essential downstream metabolic mediator of oncogenic Ras (Telang et al., 2006). Importantly, we demonstrate that PTEN elevation triggers PFKFB3 degradation through the APC/Cdh1 complex. Super-PTEN cells show reduced protein levels of PFKFB3, with no changes at the mRNA level. Beyond the PTEN-dependent inhibition of glycolysis, we find that Super-PTEN cells have reduced levels of GLS, the first enzyme in glutaminolysis. Once again, this key tumor-suppressive metabolic switch that opposes glutaminolysis is triggered by PTEN elevation through GLS degradation by the APC/Cdh1 complex. Interestingly, GLS has been reported to have increased activity in several tumor types, and it is upregulated in c-Myc-transformed cells (Gao et al., 2009; Wise et al., 2008), highlighting it as a potential therapeutic target.

In summary, our data unexpectedly identify PTEN as a key node for the control of obesity and tumorigenesis. Super-PTEN mice exhibit an unexpected cancer-resistant and unique metabolic state, which is the outcome of the ability of PTEN to regulate metabolism at multiple levels both from the cytosol and from the nucleus. On the one hand, these mice exhibit increased oxygen consumption and energy expenditure. On the other

hand, Super-PTEN mice and cells are less prone to transformation and cancer development. Thus, the features observed in Super-PTEN mice and cells resemble an "anti-Warburg state," in which less glucose is taken up but is more efficiently directed to the mitochondrial tricarboxylic acid cycle. Moreover, PTEN elevations induce mitochondrial biogenesis and thus increased mitochondrial ATP production. Thus PTEN couples mitochondrial function and dynamics to cellular metabolism through PI3K-dependent and PI3K-independent mechanisms. It is tempting to speculate that the unique metabolic state resulting from PTEN elevation contributes to the increased cancer resistance observed in these mice and cells by opposing cancer-associated metabolic reprogramming (Figure 7). PTEN elevation hence represents a potentially attractive therapeutic approach that could both prevent cancer development and increase energy expenditure to oppose fat accumulation and obesity.

EXPERIMENTAL PROCEDURES

Please refer to the Extended Experimental Procedures for more extensive information.

BAC Transgenesis
For transgenesis, a large genomic insert (218.50 Kb) containing the entire *Pten* locus and cloned into the BAC vector pBACe3.6 was isolated from a mouse BAC genomic library (BAC RP23-215F15 clone; RPCI library, C57BL/6J). After digestion with AscI, linearized BAC DNA was used for microinjection into the pronuclei of fertilized oocytes, derived from intercrosses between (C57BL/6 × CBA)F1 mice.

shRNAs
WT and Super-PTEN MEFs were infected with lentiviruses expressing shRNA against mouse *Cdh1* (clone ID TRCN0000027712, Open Biosystems) or rat *Tsc2* or corresponding control shRNA against luciferase (Di Nardo et al., 2009). To prepare lentiviral particles, 3×10^6 293T cells were plated per 10 cm culture dish, and then shRNAs transfected with Lipofectamine 2000 (Invitrogen). For infection, MEFs were plated at a density of 6×10^5 cells per 10 cm culture dish and infected by virus from 293T cells 48 hr after transfection. After reseeding, MEFs were used for the different assays.

In Vivo Ubiquitination Assay
PTEN-deficient PC-3 cells were transfected with a combination of pCMV6-XL4-GLS (SC114750: OriGene), HA-PTEN, Myc-CDH1, and His-ubiquitin (Ub). His-Ub-conjugated GLS was purified from cell lysates using an Ni^{2+}-NTA spin column (QIAGEN) under denaturing conditions. The extent of ubiquitination was then analyzed by immunoblotting.

Chemical Carcinogenesis
For 3MC-induced carcinogenesis, 4-month-old mice received a single intramuscular injection into one of their rear legs of a 100 μl solution containing 3-methyl-cholanthrene (Sigma), dissolved at a final concentration of 10 μg/μl in sesame oil (Sigma) as previously described (García-Cao et al., 2002; Wexler and Rosenberg, 1979).

Measurement of Oxygen Consumption
For oxygen consumption, 2×10^4 cells were plated, and 24 hr later, oxygen consumption rate (OCR) was measured with the Seahorse XF24 instrument (Seahorse Bioscience) under basal conditions and after addition of oligomycin (1 μM), FCCP (2.5 μM), and Rotenone (1 μM). All the chemicals were purchased from Sigma.

Measurement of Glucose, Lactate, and Glutamine
Glucose, lactate, and glutamine levels in culture media were measured using the BioProfile FLEX analyzer (NOVA biomedical) and normalized to cell number. Fresh media were added to a 6-well plate of cells and analyzed after 24 hr (triplicate samples).

Measurement of ROS Production
ROS production was measured by flow cytometric assessment of DCF (2′,7′-dichlorodihydrofluorescein) fluorescence. The details of this assay are described in the Extended Experimental Procedures.

FAO
FAO was determined by measuring ^3H_2O produced during cellular oxidation of [^3H] palmitate (Finck et al., 2006; Gerhart-Hines et al., 2007). Please refer to the Extended Experimental Procedures for details.

Lipid Synthesis Assay
Lipid synthesis was assayed by measuring the amount of ^{14}C incorporated into lipids after 2 hr incubation with [6-^{14}C]glucose (Hatzivassiliou et al., 2005). Please refer to the Extended Experimental Procedures for details.

Statistical Analysis
In vitro and in vivo data were analyzed with an unpaired t test (GraphPad Prism, GraphPad Software Inc.). Values of $p < 0.05$ were considered statistically significant (*$p < 0.05$; **$p < 0.01$; ***$p < 0.001$). Correlation analysis was performed with SigmaPlot 5.0 software (SPSS Inc.).

ACCESSION NUMBERS

Microarray data have been deposited in MIAME under accession number GSE35670.

SUPPLEMENTAL INFORMATION

Supplemental Information includes Extended Experimental Procedures and five figures and can be found with this article online at doi:10.1016/j.cell.2012.02.030.

REFERENCES

Alimonti, A., Carracedo, A., Clohessy, J.G., Trotman, L.C., Nardella, C., Egia, A., Salmena, L., Sampieri, K., Haveman, W.J., Brogi, E., et al. (2010). Subtle variations in Pten dose determine cancer susceptibility. Nat. Genet. *42*, 454–458.

Altenberg, B., and Greulich, K.O. (2004). Genes of glycolysis are ubiquitously overexpressed in 24 cancer classes. Genomics *84*, 1014–1020.

Atsumi, T., Chesney, J., Metz, C., Leng, L., Donnelly, S., Makita, Z., Mitchell, R., and Bucala, R. (2002). High expression of inducible 6-phosphofructo-2-kinase/fructose-2,6-bisphosphatase (iPFK-2; PFKFB3) in human cancers. Cancer Res. *62*, 5881–5887.

Banito, A., Rashid, S.T., Acosta, J.C., Li, S., Pereira, C.F., Geti, I., Pinho, S., Silva, J.C., Azuara, V., Walsh, M., et al. (2009). Senescence impairs successful reprogramming to pluripotent stem cells. Genes Dev. *23*, 2134–2139.

Banito, A., and Gil, J. (2010). Induced pluripotent stem cells and senescence: learning the biology to improve the technology. EMBO Rep. *11*, 353–359.

Böhni, R., Riesgo-Escovar, J., Oldham, S., Brogiolo, W., Stocker, H., Andruss, B.F., Beckingham, K., and Hafen, E. (1999). Autonomous control of cell and organ size by CHICO, a Drosophila homolog of vertebrate IRS1-4. Cell *97*, 865–875.

Bonneau, D., and Longy, M. (2000). Mutations of the human PTEN gene. Hum. Mutat. *16*, 109–122.

Cantley, L.C., and Neel, B.G. (1999). New insights into tumor suppression: PTEN suppresses tumor formation by restraining the phosphoinositide 3-kinase/AKT pathway. Proc. Natl. Acad. Sci. USA *96*, 4240–4245.

Christofk, H.R., Vander Heiden, M.G., Harris, M.H., Ramanathan, A., Gerszten, R.E., Wei, R., Fleming, M.D., Schreiber, S.L., and Cantley, L.C. (2008). The M2 splice isoform of pyruvate kinase is important for cancer metabolism and tumour growth. Nature *452*, 230–233.

Clower, C.V., Chatterjee, D., Wang, Z., Cantley, L.C., Vander Heiden, M.G., and Krainer, A.R. (2010). The alternative splicing repressors hnRNP A1/A2 and PTB influence pyruvate kinase isoform expression and cell metabolism. Proc. Natl. Acad. Sci. USA *107*, 1894–1899.

Colombo, S.L., Palacios-Callender, M., Frakich, N., De Leon, J., Schmitt, C.A., Boorn, L., Davis, N., and Moncada, S. (2010). Anaphase-promoting complex/cyclosome-Cdh1 coordinates glycolysis and glutaminolysis with transition to S phase in human T lymphocytes. Proc. Natl. Acad. Sci. USA *107*, 18868–18873.

David, C.J., Chen, M., Assanah, M., Canoll, P., and Manley, J.L. (2010). HnRNP proteins controlled by c-Myc deregulate pyruvate kinase mRNA splicing in cancer. Nature *463*, 364–368.

Deberardinis, R.J., Lum, J.J., and Thompson, C.B. (2006). Phosphatidylinositol 3-kinase-dependent modulation of carnitine palmitoyltransferase 1A expression regulates lipid metabolism during hematopoietic cell growth. J. Biol. Chem. *281*, 37372–37380.

DeBerardinis, R.J., Lum, J.J., Hatzivassiliou, G., and Thompson, C.B. (2008). The biology of cancer: metabolic reprogramming fuels cell growth and proliferation. Cell Metab. *7*, 11–20.

Denko, N.C. (2008). Hypoxia, HIF1 and glucose metabolism in the solid tumour. Nat. Rev. Cancer *8*, 705–713.

Di Cristofano, A., Pesce, B., Cordon-Cardo, C., and Pandolfi, P.P. (1998). Pten is essential for embryonic development and tumour suppression. Nat. Genet. *19*, 348–355.

Di Nardo, A., Kramvis, I., Cho, N., Sadowski, A., Meikle, L., Kwiatkowski, D.J., and Sahin, M. (2009). Tuberous sclerosis complex activity is required to control neuronal stress responses in an mTOR-dependent manner. J. Neurosci. *29*, 5926–5937.

Eng, C. (2003). PTEN: one gene, many syndromes. Hum. Mutat. *22*, 183–198.

Engelman, J.A., Luo, J., and Cantley, L.C. (2006). The evolution of phosphatidylinositol 3-kinases as regulators of growth and metabolism. Nat. Rev. Genet. *7*, 606–619.

Finck, B.N., Gropler, M.C., Chen, Z., Leone, T.C., Croce, M.A., Harris, T.E., Lawrence, J.C., Jr., and Kelly, D.P. (2006). Lipin 1 is an inducible amplifier of the hepatic PGC-1alpha/PPARalpha regulatory pathway. Cell Metab. *4*, 199–210.

Gao, P., Tchernyshyov, I., Chang, T.C., Lee, Y.S., Kita, K., Ochi, T., Zeller, K.I., De Marzo, A.M., Van Eyk, J.E., Mendell, J.T., and Dang, C.V. (2009). c-Myc suppression of miR-23a/b enhances mitochondrial glutaminase expression and glutamine metabolism. Nature *458*, 762–765.

Gao, X., Neufeld, T.P., and Pan, D. (2000). Drosophila PTEN regulates cell growth and proliferation through PI3K-dependent and -independent pathways. Dev. Biol. *221*, 404–418.

García-Cao, I., García-Cao, M., Martín-Caballero, J., Criado, L.M., Klatt, P., Flores, J.M., Weill, J.C., Blasco, M.A., and Serrano, M. (2002). "Super p53" mice exhibit enhanced DNA damage response, are tumor resistant and age normally. EMBO J. *21*, 6225–6235.

Gerhart-Hines, Z., Rodgers, J.T., Bare, O., Lerin, C., Kim, S.H., Mostoslavsky, R., Alt, F.W., Wu, Z., and Puigserver, P. (2007). Metabolic control of muscle mitochondrial function and fatty acid oxidation through SIRT1/PGC-1alpha. EMBO J. *26*, 1913–1923.

Goberdhan, D.C., Paricio, N., Goodman, E.C., Mlodzik, M., and Wilson, C. (1999). Drosophila tumor suppressor PTEN controls cell size and number by antagonizing the Chico/PI3-kinase signaling pathway. Genes Dev. *13*, 3244–3258.

Gregory, M.A., Qi, Y., and Hann, S.R. (2003). Phosphorylation by glycogen synthase kinase-3 controls c-myc proteolysis and subnuclear localization. J. Biol. Chem. *278*, 51606–51612.

Griffiths, E.J., and Rutter, G.A. (2009). Mitochondrial calcium as a key regulator of mitochondrial ATP production in mammalian cells. Biochim. Biophys. Acta *1787*, 1324–1333.

Hatzivassiliou, G., Zhao, F., Bauer, D.E., Andreadis, C., Shaw, A.N., Dhanak, D., Hingorani, S.R., Tuveson, D.A., and Thompson, C.B. (2005). ATP citrate lyase inhibition can suppress tumor cell growth. Cancer Cell *8*, 311–321.

Hong, H., Takahashi, K., Ichisaka, T., Aoi, T., Kanagawa, O., Nakagawa, M., Okita, K., and Yamanaka, S. (2009). Suppression of induced pluripotent stem cell generation by the p53-p21 pathway. Nature *460*, 1132–1135.

Huang, H., Potter, C.J., Tao, W., Li, D.M., Brogiolo, W., Hafen, E., Sun, H., and Xu, T. (1999). PTEN affects cell size, cell proliferation and apoptosis during Drosophila eye development. Development *126*, 5365–5372.

Hue, L., and Rider, M.H. (1987). Role of fructose 2,6-bisphosphate in the control of glycolysis in mammalian tissues. Biochem. J. *245*, 313–324.

Johnston, L.A., Prober, D.A., Edgar, B.A., Eisenman, R.N., and Gallant, P. (1999). Drosophila myc regulates cellular growth during development. Cell *98*, 779–790.

Jones, R.M., Branda, J., Johnston, K.A., Polymenis, M., Gadd, M., Rustgi, A., Callanan, L., and Schmidt, E.V. (1996). An essential E box in the promoter of the gene encoding the mRNA cap-binding protein (eukaryotic initiation factor 4E) is a target for activation by c-myc. Mol. Cell. Biol. *16*, 4754–4764.

Kawamura, T., Suzuki, J., Wang, Y.V., Menendez, S., Morera, L.B., Raya, A., Wahl, G.M., and Izpisúa Belmonte, J.C. (2009). Linking the p53 tumour suppressor pathway to somatic cell reprogramming. Nature *460*, 1140–1144.

King, A., and Gottlieb, E. (2009). Glucose metabolism and programmed cell death: an evolutionary and mechanistic perspective. Curr. Opin. Cell Biol. *21*, 885–893.

Leevers, S.J., Vanhaesebroeck, B., and Waterfield, M.D. (1999). Signalling through phosphoinositide 3-kinases: the lipids take centre stage. Curr. Opin. Cell Biol. *11*, 219–225.

Li, H., Collado, M., Villasante, A., Strati, K., Ortega, S., Cañamero, M., Blasco, M.A., and Serrano, M. (2009). The Ink4/Arf locus is a barrier for iPS cell reprogramming. Nature *460*, 1136–1139.

Li, M., Shin, Y.H., Hou, L., Huang, X., Wei, Z., Klann, E., and Zhang, P. (2008). The adaptor protein of the anaphase promoting complex Cdh1 is essential in maintaining replicative lifespan and in learning and memory. Nat. Cell Biol. *10*, 1083–1089.

Li, X., Monks, B., Ge, Q., and Birnbaum, M.J. (2007). Akt/PKB regulates hepatic metabolism by directly inhibiting PGC-1alpha transcription coactivator. Nature *447*, 1012–1016.

Liu, W.B., Ao, L., Zhou, Z.Y., Cui, Z.H., Zhou, Y.H., Yuan, X.Y., Xiang, Y.L., Cao, J., and Liu, J.Y. (2010). CpG island hypermethylation of multiple tumor suppressor genes associated with loss of their protein expression during rat lung carcinogenesis induced by 3-methylcholanthrene and diethylnitrosamine. Biochem. Biophys. Res. Commun. *402*, 507–514.

Maehama, T., and Dixon, J.E. (1998). The tumor suppressor, PTEN/MMAC1, dephosphorylates the lipid second messenger, phosphatidylinositol 3,4,5-trisphosphate. J. Biol. Chem. *273*, 13375–13378.

Marión, R.M., Strati, K., Li, H., Murga, M., Blanco, R., Ortega, S., Fernandez-Capetillo, O., Serrano, M., and Blasco, M.A. (2009). A p53-mediated DNA damage response limits reprogramming to ensure iPS cell genomic integrity. Nature *460*, 1149–1153.

Marroquin, L.D., Hynes, J., Dykens, J.A., Jamieson, J.D., and Will, Y. (2007). Circumventing the Crabtree effect: replacing media glucose with galactose

increases susceptibility of HepG2 cells to mitochondrial toxicants. Toxicol. Sci. *97*, 539–547.

Najafov, A., and Alessi, D.R. (2010). Uncoupling the Warburg effect from cancer. Proc. Natl. Acad. Sci. USA *107*, 19135–19136.

Podsypanina, K., Ellenson, L.H., Nemes, A., Gu, J., Tamura, M., Yamada, K.M., Cordon-Cardo, C., Catoretti, G., Fisher, P.E., and Parsons, R. (1999). Mutation of Pten/Mmac1 in mice causes neoplasia in multiple organ systems. Proc. Natl. Acad. Sci. USA *96*, 1563–1568.

Puigserver, P., and Spiegelman, B.M. (2003). Peroxisome proliferator-activated receptor-gamma coactivator 1 alpha (PGC-1 alpha): transcriptional coactivator and metabolic regulator. Endocr. Rev. *24*, 78–90.

Ravitz, M.J., Chen, L., Lynch, M., and Schmidt, E.V. (2007). c-myc Repression of TSC2 contributes to control of translation initiation and Myc-induced transformation. Cancer Res. *67*, 11209–11217.

Ruderman, N., and Flier, J.S. (2001). Cell biology. Chewing the fat—ACC and energy balance. Science *291*, 2558–2559.

Salmena, L., Carracedo, A., and Pandolfi, P.P. (2008). Tenets of PTEN tumor suppression. Cell *133*, 403–414.

Scanga, S.E., Ruel, L., Binari, R.C., Snow, B., Stambolic, V., Bouchard, D., Peters, M., Calvieri, B., Mak, T.W., Woodgett, J.R., and Manoukian, A.S. (2000). The conserved PI3'K/PTEN/Akt signaling pathway regulates both cell size and survival in Drosophila. Oncogene *19*, 3971–3977.

Sears, R., Nuckolls, F., Haura, E., Taya, Y., Tamai, K., and Nevins, J.R. (2000). Multiple Ras-dependent phosphorylation pathways regulate Myc protein stability. Genes Dev. *14*, 2501–2514.

Simpson, L., and Parsons, R. (2001). PTEN: life as a tumor suppressor. Exp. Cell Res. *264*, 29–41.

Song, M.S., Carracedo, A., Salmena, L., Song, S.J., Egia, A., Malumbres, M., and Pandolfi, P.P. (2011). Nuclear PTEN regulates the APC-CDH1 tumor-suppressive complex in a phosphatase-independent manner. Cell *144*, 187–199.

Suzuki, A., de la Pompa, J.L., Stambolic, V., Elia, A.J., Sasaki, T., del Barco Barrantes, I., Ho, A., Wakeham, A., Itie, A., Khoo, W., et al. (1998). High cancer susceptibility and embryonic lethality associated with mutation of the PTEN tumor suppressor gene in mice. Curr. Biol. *8*, 1169–1178.

Tee, A.R., and Blenis, J. (2005). mTOR, translational control and human disease. Semin. Cell Dev. Biol. *16*, 29–37.

Telang, S., Yalcin, A., Clem, A.L., Bucala, R., Lane, A.N., Eaton, J.W., and Chesney, J. (2006). Ras transformation requires metabolic control by 6-phos-phofructo-2-kinase. Oncogene *25*, 7225–7234.

Tennant, D.A., Durán, R.V., Boulahbel, H., and Gottlieb, E. (2009). Metabolic transformation in cancer. Carcinogenesis *30*, 1269–1280.

Tennant, D.A., Durán, R.V., and Gottlieb, E. (2010). Targeting metabolic transformation for cancer therapy. Nat. Rev. Cancer *10*, 267–277.

Tong, X., Zhao, F., and Thompson, C.B. (2009). The molecular determinants of de novo nucleotide biosynthesis in cancer cells. Curr. Opin. Genet. Dev. *19*, 32–37.

Trotman, L.C., Niki, M., Dotan, Z.A., Koutcher, J.A., Di Cristofano, A., Xiao, A., Khoo, A.S., Roy-Burman, P., Greenberg, N.M., Van Dyke, T., et al. (2003). Pten dose dictates cancer progression in the prostate. PLoS Biol. *1*, E59.

Trumpp, A., Refaeli, Y., Oskarsson, T., Gasser, S., Murphy, M., Martin, G.R., and Bishop, J.M. (2001). c-Myc regulates mammalian body size by controlling cell number but not cell size. Nature *414*, 768–773.

Utikal, J., Polo, J.M., Stadtfeld, M., Maherali, N., Kulalert, W., Walsh, R.M., Khalil, A., Rheinwald, J.G., and Hochedlinger, K. (2009). Immortalization eliminates a roadblock during cellular reprogramming into iPS cells. Nature *460*, 1145–1148.

Vander Heiden, M.G., Cantley, L.C., and Thompson, C.B. (2009). Understanding the Warburg effect: the metabolic requirements of cell proliferation. Science *324*, 1029–1033.

Vander Heiden, M.G., Locasale, J.W., Swanson, K.D., Sharfi, H., Heffron, G.J., Amador-Noguez, D., Christofk, H.R., Wagner, G., Rabinowitz, J.D., Asara, J.M., and Cantley, L.C. (2010). Evidence for an alternative glycolytic pathway in rapidly proliferating cells. Science *329*, 1492–1499.

Verdu, J., Buratovich, M.A., Wilder, E.L., and Birnbaum, M.J. (1999). Cell-autonomous regulation of cell and organ growth in Drosophila by Akt/PKB. Nat. Cell Biol. *1*, 500–506.

Warburg, O. (1956). On the origin of cancer cells. Science *123*, 309–314.

Weinkove, D., Neufeld, T.P., Twardzik, T., Waterfield, M.D., and Leevers, S.J. (1999). Regulation of imaginal disc cell size, cell number and organ size by Drosophila class I(A) phosphoinositide 3-kinase and its adaptor. Curr. Biol. *9*, 1019–1029.

West, M.J., Stoneley, M., and Willis, A.E. (1998). Translational induction of the c-myc oncogene via activation of the FRAP/TOR signalling pathway. Oncogene *17*, 769–780.

Wexler, H., and Rosenberg, S.A. (1979). Pulmonary metastases from autochthonous 3-methylcholanthrene-induced murine tumors. J. Natl. Cancer Inst. *63*, 1393–1395.

Wise, D.R., DeBerardinis, R.J., Mancuso, A., Sayed, N., Zhang, X.Y., Pfeiffer, H.K., Nissim, I., Daikhin, E., Yudkoff, M., McMahon, S.B., and Thompson, C.B. (2008). Myc regulates a transcriptional program that stimulates mitochondrial glutaminolysis and leads to glutamine addiction. Proc. Natl. Acad. Sci. USA *105*, 18782–18787.

Wu, Z., Puigserver, P., Andersson, U., Zhang, C., Adelmant, G., Mootha, V., Troy, A., Cinti, S., Lowell, B., Scarpulla, R.C., and Spiegelman, B.M. (1999). Mechanisms controlling mitochondrial biogenesis and respiration through the thermogenic coactivator PGC-1. Cell *98*, 115–124.

Zhang, H., Cicchetti, G., Onda, H., Koon, H.B., Asrican, K., Bajraszewski, N., Vazquez, F., Carpenter, C.L., and Kwiatkowski, D.J. (2003). Loss of Tsc1/Tsc2 activates mTOR and disrupts PI3K-Akt signaling through downregulation of PDGFR. J. Clin. Invest. *112*, 1223–1233.

Zoncu, R., Efeyan, A., and Sabatini, D.M. (2011). mTOR: from growth signal integration to cancer, diabetes and ageing. Nat. Rev. Mol. Cell Biol. *12*, 21–35.

Zundel, W., Schindler, C., Haas-Kogan, D., Koong, A., Kaper, F., Chen, E., Gottschalk, A.R., Ryan, H.E., Johnson, R.S., Jefferson, A.B., et al. (2000). Loss of PTEN facilitates HIF-1-mediated gene expression. Genes Dev. *14*, 391–396.